

Article

Not peer-reviewed version

Sphere Packing in 2 1/2 Dimensions

[Kenneth Stephenson](#) *

Posted Date: 10 February 2026

doi: 10.20944/preprints202602.0810.v1

Keywords: sphere packing; packing density; rigidity; bucktubes



Preprints.org is a free multidisciplinary platform providing preprint service that is dedicated to making early versions of research outputs permanently available and citable. Preprints posted at Preprints.org appear in Web of Science, Crossref, Google Scholar, Scilit, Europe PMC.

Copyright: This open access article is published under a [Creative Commons CC BY 4.0 license](#), which permit the free download, distribution, and reuse, provided that the author and preprint are cited in any reuse.

Disclaimer/Publisher's Note: The statements, opinions, and data contained in all publications are solely those of the individual author(s) and contributor(s) and not of MDPI and/or the editor(s). MDPI and/or the editor(s) disclaim responsibility for any injury to people or property resulting from any ideas, methods, instructions, or products referred to in the content.

Article

Sphere Packings in $2\frac{1}{2}$ Dimensions

Kenneth Stephenson 

University of Tennessee, Knoxville; kstephe2@utk.edu

Abstract

This paper investigates cylindrical sphere packings, that is, patterns of uniform spheres with mutually disjoint interiors which are all tangent to a common cylinder. The key unifying themes are existence and uniqueness of hexagonal packings, in which each sphere is tangent to six others. Constructions are both intuitive and subtle, but result in the complete characterization in term of integer parameter pairs (m, n) . Interesting questions in rigidity and density are encountered. Density questions arise because the packings, being of equal diameter, lie within the space between inner and outer cylinders. This density problem hovers between the 2D and 3D sphere packing cases, and though it is not solved here, it is conjectured that the hexagonal packings are densest for the countable number of cylinders which support them. Other geometric objects are along for the ride, including equilateral triangles and the packings' dual graphs, which are associated with patterns of carbon atoms forming buckytubes. Interesting structural rigidity questions also arise.

Keywords: sphere packing; packing density; rigidity; buckytubes

Introduction

This is a paper about sphere packings on cylinders in 3-space. That is, infinite configurations of congruent spheres with mutually disjoint interiors which are all tangent to the outside of a given cylinder. Figure 1 will set the scene.

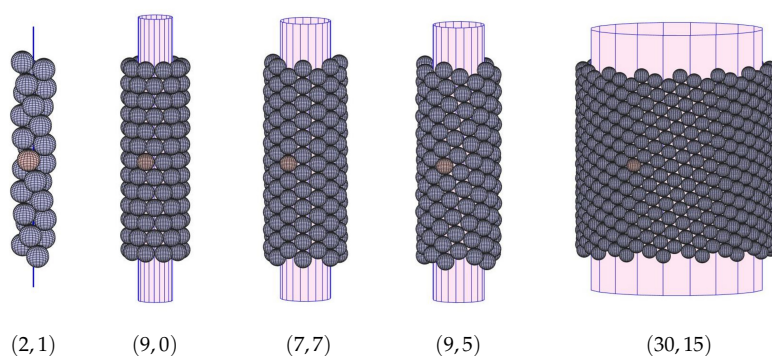


Figure 1. Hexagonal cylindrical sphere packings (truncated for display).

The objects involved here, spheres and cylinders, are so familiar that the reader is encouraged to imagine hands-on constructions — or actually *do* hands-on constructions, as the author has enjoyed with undergraduate students. Getting started is only slightly more difficult than it would appear: Figure 1 illustrates *hexagonal* packings, in which each sphere is tangent to six others. These play the central role in our story here, and despite their simple and pleasing visual nature, characterizing these packings faces engaging challenges. Combinatorics enters in a crucial way, with abstract triangulations representing patterns of sphere tangency. These can be realized concretely using yet another familiar, manipulable object, the flat equilateral triangle. Figure 2 illustrates the triangulations behind three of the packings from Figure 1; they are realized as cylindrical polyhedra formed by equilateral triangles, each associated with a triple of mutually tangent spheres.

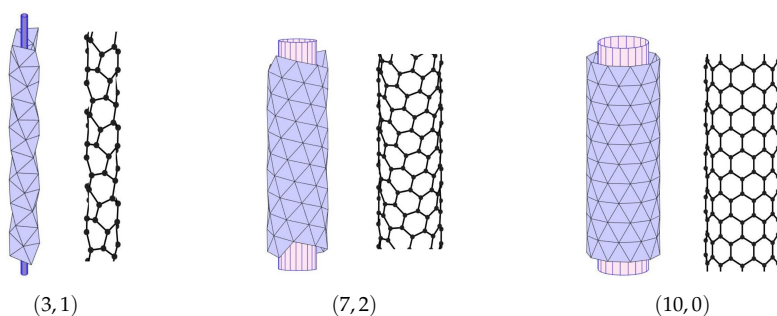


Figure 2. Samples of cylindrical polyhedra and dual buckytubes associated with hCSP's.

Figure 2 also illustrates what nature produces with its own manipulations: paired with the polyhedra are the familiar patterns of buckytubes, representing carbon atoms and their bonds. The combinatorics of buckytubes are in one-to-one correspondence with the duals of triangulations of hexagonal sphere packings. Our interests here are geometric, but there may well be concrete applications in the study of carbon structures, which are of great interest in physics and material science. The packings themselves are of scientific interest, as they are common in modeling of many natural columnar structures, from plant cells, to foams, crystals, and nanoparticles. The term “sphere packing” will, for many readers, raise the issue of packing *density*. In our case, the spheres have the same diameter, so they lie in the space between two cylinders. How much of the volume can they occupy? Our discussion of density questions shows that there is much work yet to be done with these cylindrical sphere packings.

Overview:

The geometric objects involved here — cylinders, spheres, triangles — are so familiar that this paper can take a top-down approach, hopefully sharing the sense of discovery which physicists enjoy but which all too often is obscured in mathematical writing. In Part A we construct sphere packings with a hexagonal themed approach — one that a reader with the right maker skills might even realize concretely. Applying thought experiments, visualization, and intuition, we reach a characterization of all cylindrical packings with hexagonal combinatorics. Part B continues the intuitive approach with a second construction of hCSP's using equilateral triangles. Although this does not provide a new proof of existence and uniqueness, it raises interesting questions in a major related topic, *rigidity* theory. In Part C, we then move to discuss packing density, a topic with a long mathematical history. That leaves Part D of the paper, where we fill in the formal, computational, and at times annoying details which justify our earlier constructions and results.

Part A: Hexagonal Packings

Let us set the environment for our constructions. We work in \mathbb{R}^3 with cylindrical coordinates (r, θ, z) . $\text{Cyl}(r)$ will denote a cylinder of radius $r \geq 0$ whose central axis is the z -axis. This will be the *inner cylinder* in packings, and one attaches spheres of diameter 1 with mutually disjoint interiors tangent to this inner cylinder. The result is called a Cylindrical Sphere Packing (CSP) on $\text{Cyl}(r)$. Spheres tangent to the outside of $\text{Cyl}(r)$ will also be tangent to the inside of the *outer cylinder* $\text{Cyl}(r + 1)$. The region between these is called the *solid cylinder* for r and is the setting for the density issue discussed in Part C. There is a crucial additional cylinder involved, the *mid cylinder* $\text{Cyl}(r + 1/2)$. This contains the centers of the spheres of the packing; since it enters nearly all our computations, we denote its radius by $R = r + 1/2$.

A.1. The Construction

There are myriad ways to build CSP's, but we will concentrate on a systematic approach based on hexagonal flowers. For a given cylinder $\text{Cyl}(r)$, start by attaching the “base” sphere S_0 at the point $(r, 0, 0)$; in most images, S_0 will appear as pale red, while the other spheres will be light blue. Attach a

sphere S_1 to $\text{Cyl}(r)$ so that it is tangent to S_0 , and then another, S_2 which is tangent to both S_0 and S_1 . (By convention, S_2 is chosen so the triple $\{S_0, S_1, S_2\}$ of mutually tangent spheres is counterclockwise oriented as viewed from outside the cylinder.) As we will see shortly, other spheres are added as the construction proceeds. Figure 3 shows the situation we have reached at this point. Obscured in the picture is the euclidean triangle formed by the centers of these three spheres; it is equilateral with unit edge lengths.

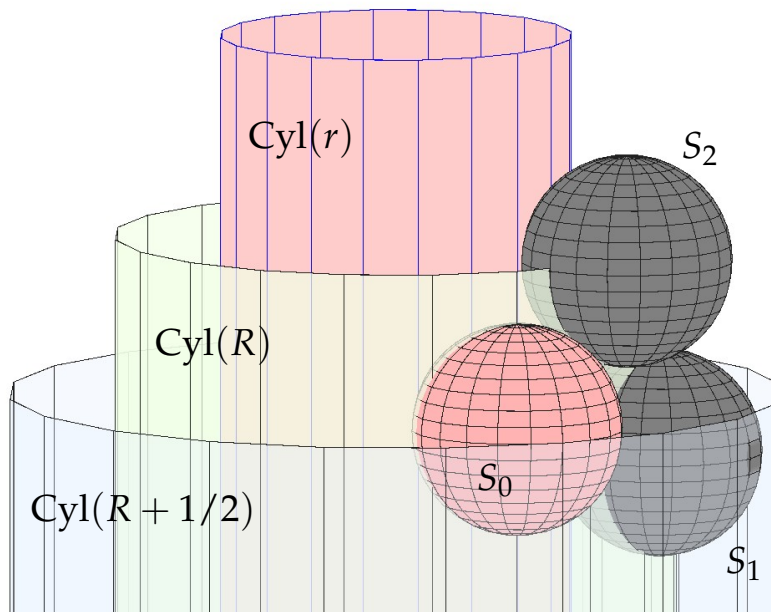


Figure 3. The inner, mid, and outer cylinders, and a tangent triple $\{S_0, S_1, S_2\}$ of spheres.

Now continue construction counterclockwise around S_0 , sphere-by-sphere: whenever a tangent triple $\{S_0, S_j, S_{j+1}\}$ is already in place, compute S_{j+2} to get the next tangent triple $\{S_0, S_{j+1}, S_{j+2}\}$.

A Pleasant Surprise: When you work your way around and are ready to position S_7 , you will find that it precisely matches S_1 ! You have completed a *hex flower* for S_0 — a pattern of 6 successively tangent spheres with mutually disjoint interiors all tangent to and surrounding the central sphere S_0 .

This closure property applies to the completion of hex flowers about any central sphere. We will prove closure in Part D, but accepting that for now, the final construction stage is a recursive process carried out *ad infinitum*: (1) Among the spheres already placed on $\text{Cyl}(r)$ at a given stage, find some tangent pair which is missing one of its shared neighbors. (2) Compute the location and put that new sphere in place. (3) Return to step (1) and repeat.

Everything is going so well, is it not? It would seem that you will complete the hex flower for every sphere, leading to a hexagonal CSP. *Voila??* — But wait; perhaps the reader has already anticipated an obstruction.

An Unpleasant Surprise? As the pattern of added spheres grows outward from S_0 , those being added to the right around the cylinder might not be compatible with those added to the left. There might be spheres whose hex flowers cannot be completed because the next tangent sphere to be added would improperly overlap a sphere already in place.

Indeed, this is the typical situation: we will see that the process will generically fail to produce a hexagonal sphere packing. Figure 4 illustrates two failed attempts starting with the same parameters:

everything looks good on the front, but you peek around the back and you see that things do not fit. The ragged gap is what you might expect; the more pleasant gap along a helix is called a *line-slip*, and we will say more about it later.

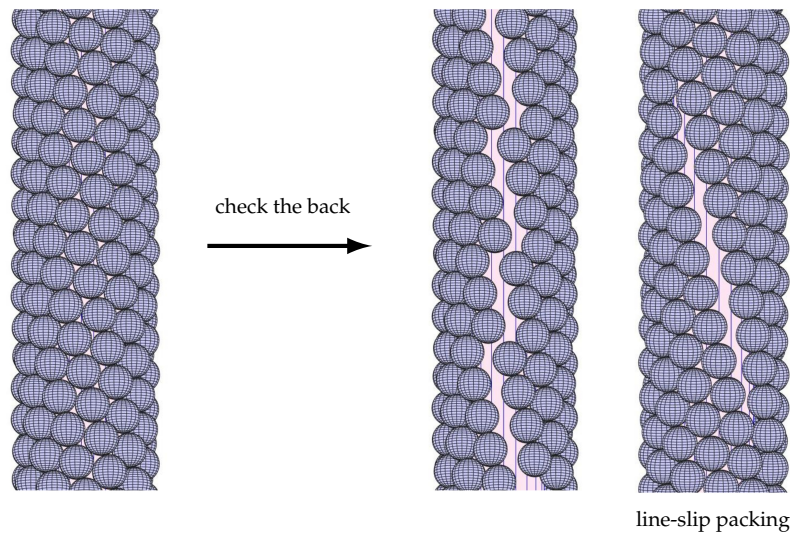


Figure 4. Construction worked? No! Ragged or line-slip gap around back.

We will have a lot to say about this construction, but let us start with issues that may have occurred to the reader. First is that the radius r might be too small for $\text{Cyl}(r)$ to support even a single hex flower, much less a hexagonal packing. That is the case, and we establish the positive lower bound $r_{\min} \sim 0.01963$ in §D.1.. Second is that due to the choices in the reiterated step (1), the resulting configuration may not be unique (see Figure 4). In fact, it will be unique if and only if it is a hexagonal packing. Our task in the next section is to identify those isolated cases in which a hexagonal packing emerges.

A.2. The Hexagonal Cases

When does this construction process succeed in building a hexagonal CSP (denoted an hCSP)? We approach this question by observing success and discovering the key parameters. All our reasoning will be proven in Part D.

So let us assume we encounter a configuration \mathcal{S} of spheres tangent to $\text{Cyl}(r)$ in which every sphere is the center of a hex flower, as with the examples in Figure 1. There is an unmistakable visual uniformity within each hCSP. There are strings of spheres forming spirals around the cylinder — indeed, there are three families of spirals (two typically stand out visually while the third may be harder to see). All the spirals from any one family will fill out the full packing. Examples are illustrated in Figure 5.

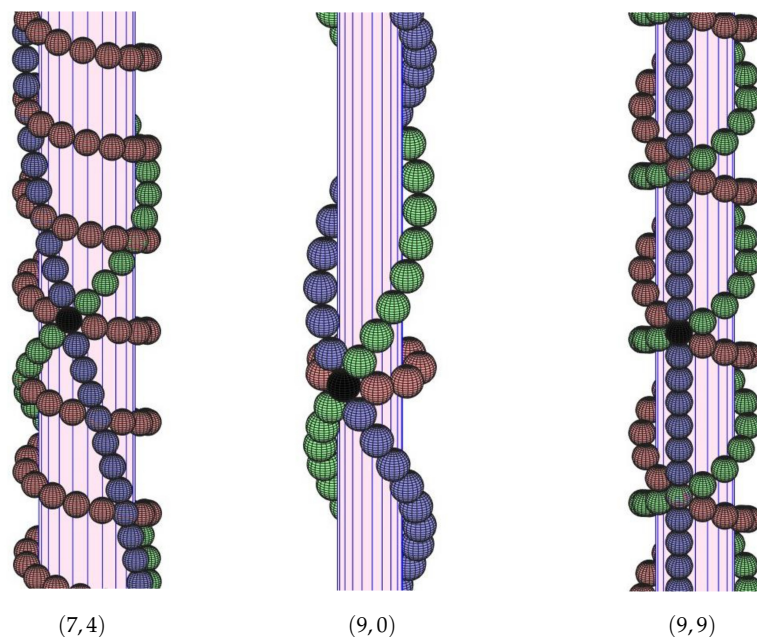


Figure 5. The three spiraling strings of tangent spheres

Focus on any spiral and note its regularity: the centers (R, θ, z) actually lie along a helical arc, hinting at an underlying isometry: combining a translation in the z direction with an associated rotation about the z -axis gives an isometry of \mathbb{R}^3 which maps each sphere of that spiral to the next. In other words, in a given spiral path, the heights z and angles θ of successive sphere centers change by constant amounts. This key observation leads us to a particular closed string of tangent spheres of special interest.

The base sphere S_0 of \mathcal{S} has a flower with a counterclockwise list $\{S_1, S_2, \dots, S_6\}$ of petals. Necessarily one of these petals, say S_1 , has height z_1 less than or equal to that of S_0 while its counterclockwise neighbor, S_2 , has height z_2 greater than S_0 . Start taking steps from S_0 along the spiral through S_0 and S_1 . There are two possibilities:

- (1) After taking some number m of steps you have returned to S_0 .
- (2) After taking m steps, you find that an additional n steps along another spiral (namely, one parallel to that through S_0 and S_2) will bring you back to S_0 .

In either case, the result is a closed string of spheres with disjoint interiors which starts and ends at S_0 . We will call this an (m, n) -necklace and we refer to the full packing \mathcal{S} as an (m, n) -hCSP. (In case (1), we take $n = 0$.)

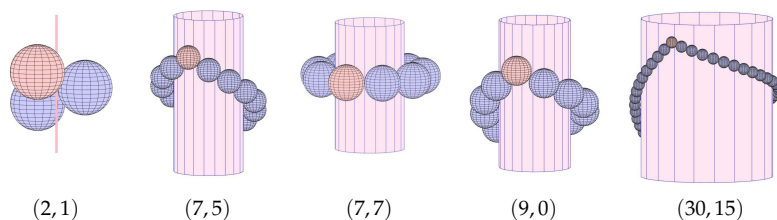


Figure 6. (m, n) -necklaces for the hCSP's of Figure 1.

As one might guess from studying Figure 6, \mathcal{S} is just an infinite stack of copies of its necklace. We exploit that in the proof of the following theorem, which shows that the pairs (m, n) serve to parametrize all hCSP's.

Theorem 1. For every pair (m, n) of integers with $m \geq n \geq 0$ and $m + n \geq 3$ there is an essentially unique radius r whose cylinder $\text{Cyl}(r)$ supports an (m, n) -hCSP. This hCSP is unique up to isometries of \mathbb{R}^3 . Moreover, every hCSP is an (m, n) -hCSP for some such pair (m, n) .

Our proof is based on observations and a dynamic thought experiment; formal justifications are in Part D, along with details on how to compute the relevant parameters.

Proof. From the given m and n , we first need to identify appropriate geometric parameters. Suppose S is a hCSP with (m, n) -necklace. Using our earlier observations, the positions of the first two spheres of the necklace, S_0 and S_1 , are enough to reconstruct the entire packing. We can arrange that S_0 is centered on the mid cylinder at $(R, 0, 0)$ and S_1 is centered at (R, θ_1, z_1) . Recall that $R = r + 1/2$ and that $z_1 \leq 0$. The only geometric parameters we need, then, are $r = r(m, n)$ and $\zeta = \zeta(m, n)$, with ζ playing the role of z_1 . We may assume henceforth that $m \geq n$; if not, one can reflect the sphere packing in the (x, y) -plane to get a CSP with the roles of m and n interchanged.

Two Special Cases: For cases $n = 0$ and $n = m$ we compute explicit r and ζ values. When $n = 0$, we have $m \geq 3$ and an $(m, 0)$ -hCSP will have a necklace of m spheres that stretches horizontally around $\text{Cyl}(r)$. The edges connecting necklace centers forms a regular unit-sided p -gon inscribed in a circle of radius R . An easy computation gives R and we conclude

$$\text{For an } (m, 0)\text{-hCSP: } r(m, 0) = \frac{1}{2 \sin(\frac{\pi}{m})} - 1/2, \quad \zeta(m, 0) = 0, \quad m \geq 3. \quad (1)$$

For an (m, m) -hCSP, we see from symmetry in the (x, y) -plane that the sphere S_1 and its tangent neighbor S_2 will have centers directly above one another, implying $\zeta = -1/2$. The sphere S neighboring S_1 and S_2 and opposite S_0 will have height 0. The line from the center of S_0 to the tangency point of S_1 and S_2 has length $\sqrt{3}/2$, as does the line from there to the center of S . Replicating around the cylinder, there will be $2m$ of these segments forming a regular $2m$ -gon inscribed in a circle of radius R , and we conclude

$$\text{For an } (m, m)\text{-hCSP: } r(m, m) = \frac{\sqrt{3}}{4 \sin(\frac{\pi}{2m})} - 1/2, \quad \zeta(m, m) = -1/2, \quad m \geq 2. \quad (2)$$

The General Case: Assuming now that $m > n > 0$, we consider a string of $m + n$ tangent spheres as though it were a string of pearls — a pearl necklace. We will be draping this necklace around a cylinder $\text{Cyl}(r)$. If r were equal to $r(m + n, 0)$, as computed earlier, then the $m + n$ pearls would form a choker about $\text{Cyl}(r)$, a tight horizontal necklace. If r were any larger, the necklace could not reach around $\text{Cyl}(r)$. On the other hand, we know there is a smallest cylinder that supports a hexagonal flower. The r we need is somewhere between these extremes.

For our thought experiment, consider decreasing r from its maximum value and watching the behavior of the necklace draped on $\text{Cyl}(r)$. First, however, we must add some rigidity: Let S denote the m^{th} pearl along the necklace. For a given r , if you gently pull S downward you will reach a point where it can physically go no lower. The tension in the necklace will then force the first m pearls to lie along a downward sloping geodesic — the shortest path along $\text{Cyl}(r)$ from S_0 to S . The remaining n pearls must lie along an upward sloping geodesic, wrapping the rest of the way around from S to S_0 . We call this particular necklace (m, n) -elegant. It is clearly unique for a given cylinder $\text{Cyl}(r)$. Since geodesic paths on cylinders are helical, this means that in an (m, n) -elegant necklace, the heights of the first m pearls drop in equal successive steps, which we will denote by $\zeta \leq 0$, while the heights of the remaining n pearls rise in equal successive steps, denoted by z_2 . It is elegant necklaces that we work with from now on.

For each $\text{Cyl}(r)$, the lowest pearl S in its (m, n) -elegant necklace is at height $m \cdot \zeta$. This lowest pearl will clearly drop in height as r decreases, so ζ becomes more negative as r decreases. But what

are we watching for? If an elegant necklace were part of a global hexagonal sphere packing, then S would be the center of a hex flower of spheres in that packing. One of its petals would be the next sphere with height increment ζ (extending the spiral direction of the first m pearls), and its neighboring petal would be the pearl after S in the necklace, with height increment z_2 . Look to the necklaces of Figure 7 to visualize the situation. For each of those $(7,4)$ -elegant necklaces, we show a green sphere S_G tangent to S with height increment ζ , while the blue sphere S_B is the $(m+1)^{\text{st}}$ pearl of the necklace itself, tangent to S with height increment z_2 .

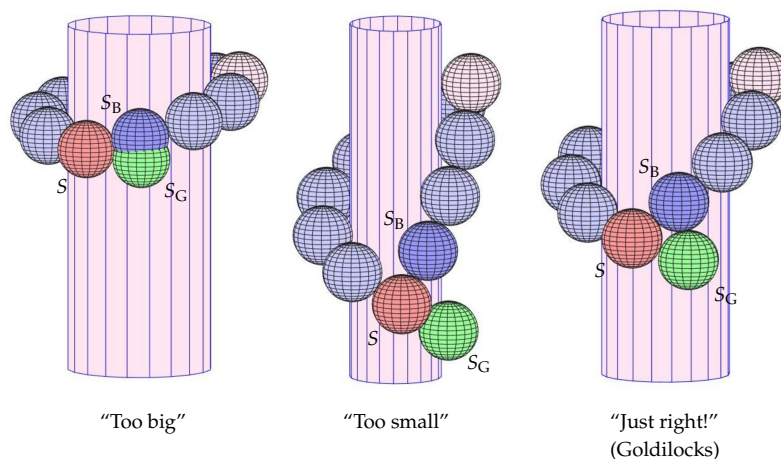


Figure 7. $(7,4)$ -elegant necklaces on various cylinders.

What you want to watch is the distance between the centers of S_G and S_B . Denote this distance by $\delta = \delta(r)$. If this necklace were part of a hexagonal packing on $\text{Cyl}(r)$, then S_G and S_B would necessarily be tangent, so $\delta(r) = 1$. This distance function δ provides our opening!

When r takes its maximum value, the necklace is a horizontal choker, S_G and S_B would be identical, and $\delta(r) = 0$. However, as suggested in Figure 7, as r decreases, S_G and S_B move apart, so $\delta(r)$ increases. Indeed, if you visualize the necklace on progressively smaller cylinders you will see it drooping until it eventually collapses — the pearls cannot remain tangent to the cylinder without beginning to overlap. At some point the pearl before S and the pearl after S in the necklace will be tangent to one another, meaning S_G and S_B must be far apart and $\delta(r) > 1$. As $\delta(r)$ is clearly a continuous function, the intermediate value theorem ensures some radius r for which $\delta(r) = 1$ and S_G and S_B are tangent. For r , this necklace is called the (m,n) -Goldilocks necklace. Once you have the (m,n) -Goldilocks necklace, our earlier construction method lets you fill out the rest of an hCSP. Indeed, stacking translated and rotated copies of the necklace will give you the full packing on $\text{Cyl}(r)$.

A closer study of $\delta(r)$ shows that the radius r for which $\delta(r) = 1$ is unique, so we will be justified in writing $r = r(m,n)$. The argument is presented in Part D, but is based on another bit of geometry: connecting the centers of S , S_G , and S_B forms a triangle in 3-space with two sides of unit length. If α denotes the angle at S in this triangle, then S_G and S_B will be tangent if and only if this triangle is equilateral, if and only if $\alpha = \pi/3$, if and only if $\cos(\alpha) = 1/2$. As it happens, as r decreases from its maximum value $r(m+n,0)$, the angle $\cos(\alpha(r))$ is strictly decreasing. Therefore, it can take the value $1/2$ only once, namely, when $r = r(m,n)$, proving uniqueness.

Summarizing, given $m > n > 0$, there is a single radius r whose (m,n) -elegant necklace is (m,n) -Goldilocks, and hence part of a (m,n) -hCSP on $\text{Cyl}(r)$. Conversely, we have observed that every hCSP contains an (m,n) -elegant necklace for some m and n , and this is clearly (m,n) -Goldilocks. Thus hCSP's are (up to isometries) in one-to-one correspondence with integer pairs (m,n) , where $m \geq n \geq 0$. \square

One consequence of this theorem is confirmation of our earlier comments: for all but countably many radii r , our construction of hex flowers on $\text{Cyl}(r)$ starting from a tangent pair S_0, S_1 will

encounter an unpleasant surprise — hex flowers that cannot be completed. In Part D we present a table containing the exceptional values $r(m, n)$, those that support hCSP's for $m = 2, 3, \dots, 13$. The reader is encouraged to see what can be gleaned from this table, recalling that only $r(m, 0)$ and $r(m, m)$ are explicit, while other entries are numerical approximations. This open question in particular may come to mind:

Open Question 1. *Does there exist a cylinder $\text{Cyl}(r)$ which supports an (m, n) -hCSP for two distinct pairs (m, n) , $m \geq n \geq 0$?*

In Part D we present, for parameters m and n , a non-linear system of two equations for r and ζ . However, as we have only numerical approximations to the solutions, this open question will be difficult to address.

Part B: Rigidity

Viewing a cylinder as simply a rolled up plane, the reader may see other ways to construct hCSP's. We discuss an appealing but naive approach that does not quite work. However, a slightly trickier one succeeds while also leading to interesting rigidity questions.

It is well known that the plane is the *universal cover* of the cylinder. We will formalize this in Part D, but as an analogy, picture rolling a cardboard tube (the cylinder) so it picks up wrapping paper (the plane) to make it easier to store. One ends up with several sheets of paper over every point of the tube, but identifying sheets over the same points as a single layer leaves just a cylinder.

With this image in mind, the reader is offered this thought experiment: Start with a close packed hexagonal lattice of uniform spheres resting on the plane. (This is just one of the planar sheets of spheres within a cannonball packing of space.) Consider $\text{Cyl}(\rho)$ as a (infinite) rolling pin which has glue on it. Start rolling across the tops of the spheres, each sphere adhering to the rolling pin as it passes by. In your mind's eye are you starting to see emergence of a CSP?

Of course, there is a difficulty we have faced before: as you keep rolling along, the spheres already adhering to the rolling pin will start to encounter new spheres still in the lattice. If the direction in which we are rolling and the radius of the rolling pin are just right, each attached sphere that encounters a new sphere will match it identically, so they just merge into one and we continue rolling along. In this instance, have we realized a hCSP? I thought so when I first imagined this process — but I was wrong! Due to the curvature of the rolling pin, spheres tangent in the plane will become separated as they are picked up. So we do *not* get a sphere packing! Still, the attempt makes clear how sensitive the construction is to the radius of the cylinder and its rolling direction, and one can see in a natural way how different helical patterns of spheres arise.

Disappointing? Perhaps, but also suggestive. Let us *unroll* an existing hCSPus \mathcal{S} and see what we learn. What we unroll, however, is the mid cylinder, since it contains the sphere centers. The centers for each triple of tangent spheres in \mathcal{S} defines a unit-sided equilateral triangle, and these attach to one another to form a cylindrical polyhedron. The whole process is depicted in Figure 8.

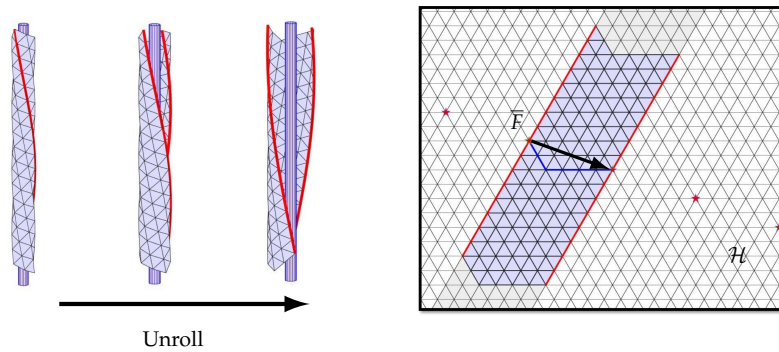


Figure 8. Unrolling a (truncated) $(4,2)$ -hCSP polyhedron.

Six triangles meet at every vertex of this polyhedron. We have cut it open along one of its spiral edge paths, and it opens up to lie perfectly flat in the plane; it becomes part of the familiar equilateral tiling of the plane, which we denote by \mathcal{H} . Note that \mathcal{H} is *not* covering the cylinder itself, but rather the cylindrical polyhedron. Our unrolling defines a fundamental region Ω in \mathcal{H} , whose opposite edges are to be identified. In Figure 8 the red stars are points associated with the center of S_0 ; the vector \bar{F} from one to the next generates the fundamental group of the covering. Especially note the blue edge path connecting successive stars: it has $m = 4$ steps along one axis and $n = 2$ along another, so \mathcal{S} is an $(4,2)$ -hCSP.

Now you may see a real opportunity to construct hCSP's by reverse engineering this unrolling — though there are some complications. The procedure starts with integers (m, n) , and a fundamental vector \bar{F} formed, as in Figure 8, with m steps along one axis and n along another in \mathcal{H} . Place a cylinder on the plane at the initial end of \bar{F} and with axis perpendicular to \bar{F} . Roll it towards the terminal end, picking up vertices as it rolls along. If you have chosen a cylinder of the proper radius r , the beginning and end of \bar{F} will find themselves at the same point on the cylinder. You have now built the polyhedron for an (m, n) -hCSP and all that is left is to place a sphere at every vertex.

This construction is quite subtle, so the reader is encouraged to spend some time visualizing the mechanics. As the vertices are picked up and triangles are added to the growing polyhedron, the structure has to crinkle up because the triangles remain connected, yet must take their various tilts. It is not easy to picture: the vertices end up on the cylinder, but the faces, to remain flat and equilateral, find themselves magically inside. You might think at first that $2\pi r = |\bar{F}|$, but the crinkled nature of the polyhedron forces r to be larger.

In the $(m, 0)$ and (m, m) cases, the mechanics are easier to visualize (and explicit radii are already known). However, as mechanically attractive as this approach to hCSP's is, there is little hope that one can prove existence and uniqueness for general (m, n) via this route.

Nevertheless, these experiments lead to another broad topic: rigidity. Picture the skeleton of an hCSP, the edges between tangent spheres, as a physical structure in space (though infinite in extent). Treat the edges as unit length bars joined at each end to 5 other bars with flexible joints. Is that structure mechanically rigid? That is, is this the only shape it can take? Figure 9 illustrates that the answer is no for (m, m) -hCSP's. For other (m, n) pairs, however, the author finds it difficult to imagine any such flexibility.

Open Question 2. *Is the skeleton for an (m, n) -hCSP rigid when $n \neq m$?*

For general reference on rigidity, the reader is directed to [5].

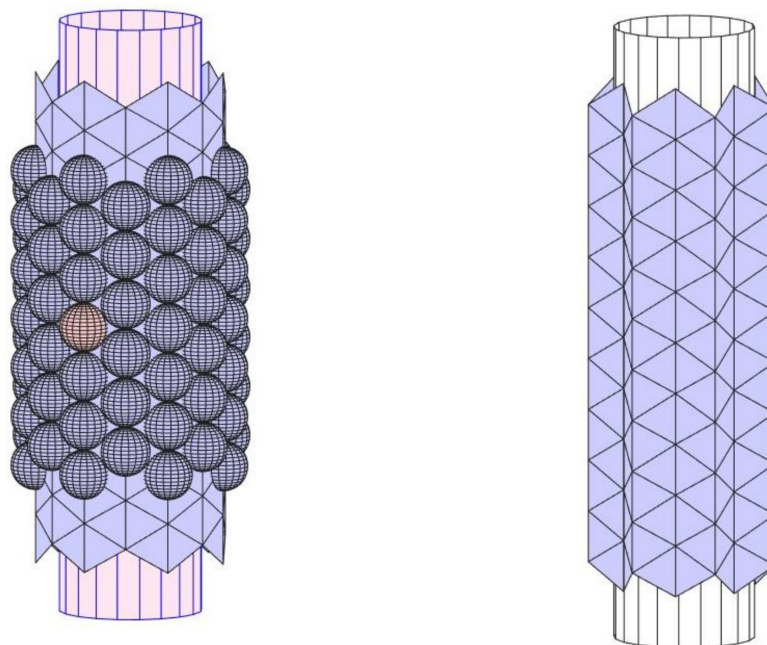


Figure 9. An (m, m) -hCSP polyhedron is not rigid.

There is one more question that might come to mind for those who know the historical importance of hexagonal combinatorics in the development of circle packing. A foundational theorem is this: *Suppose \mathcal{P} is a collection of circles in the plane having mutually disjoint interiors and a tangency graph that forms a hexagonal triangulation of the plane. Then all circles of \mathcal{P} must have the same radius. I.e., it is a penny packing.* See [11]. This suggests the following conjecture, which we will not pursue here:

Conjecture 1. *Suppose \mathcal{S} is a configuration of spheres tangent to a common cylinder having mutually disjoint interiors and a tangency graph that forms a hexagonal triangulation of the cylinder. Then all spheres of \mathcal{S} have the same radius.*

In other words, up to a scaling factor, \mathcal{S} must be one of our hCSP's. The limiting case of the conjecture, when $r = \infty$ and the cylinder becomes a plane, would, if true, be a direct extension of the penny packing result for circles in the plane.

(Incidentally, the topic of circle packing, initiated by Bill Thurston [13], is in general quite distinct from sphere packing; the reader is referred to [12]. For an additional work motivating this conjecture, see the paper [1] about Doyle spiral circle packings.)

Part C: Packing Density

The topic of “sphere packing” is surprisingly broad and has a mathematical history reaching back two millennia: what is the densest arrangement of congruent spheres in a given region, that is, the arrangement that takes up the greatest proportion of the volume? The dimension 2 and 3 cases are most familiar. In the plane, the “penny packing”, a hexagonal arrangement of congruent discs, is easily proven to maximize area density. However, the step to dimension 3 is far from easy. In fact, the famous Kepler Conjecture of 1611 proposed that in 3-space, the “cannonball packing” would maximize volume density. This was only proven in 1998 by Thomas Hales [6]. Again there is a hexagonal character to the pattern because the spheres are arranged in planar sheets, like the penny packing of discs, which are then stacked atop one another. Mathematicians have, of course, pushed to higher dimension, where the results are even more challenging. The density problem remains open except for dimensions 8 and 24, where the answers have earned Maryna Viazovska the Fields Medal in 2022. These provide the basis for important error correcting codes (see [3,4]).

For cylindrical sphere packings, the issue hovers somewhere between the 2 and 3 dimensional cases: we might call it 2 and 1/2 dimensional — the spheres live in 3D space hugging a 2D surface. What is the sphere packing that occupies the greatest proportion of the volume of the solid cylinder about $\text{Cyl}(r)$?

Spheres tangent to $\text{Cyl}(r)$ are also tangent to the *inside* of $\text{Cyl}(r + 1)$, and there has been research in the physics literature about density of packings *within* cylinders. These questions arises in various natural and physical situations, with cylinders containing cells, crystals, soft spheres, or foams, for example. See [2,8,9] and works cited there. These studies often model systems on solid spheres and their critical parameter is D/d , the ratio of the diameter of the cylinder to that of the spheres. For D/d less than roughly 2.715, simulations suggest that the densest packing will have all spheres tangent to the cylinder wall, while for larger values of D/d there may be spheres interior to the cylinder. This D/d cutoff converts to $r < 0.3574$ in our setting, and from Table 1 one can see that the (2, 1)-, (2, 2)-, (3, 2)-, (4, 1)-, and (5, 0)-hCSP's fall within this setting. The work by physicists has been largely based on simulations, both physical and computer based, along with numerical approximations and analytic searches. Though this work consistently shows that nature prefers the hexagonal motif, purely mathematical claims about density remain open.

Suppose \mathcal{S} is a CSP on $\text{Cyl}(r)$. Since the solid cylinder about $\text{Cyl}(r)$ has infinite volume, a natural way to define density takes the limit of densities in truncated cylinders. (Density is also called “average density” or “packing fraction”.)

For $h > 0$, let n be the number of spheres with centers having height z in $[-h, h]$. We then define the pre-density and density as

$$\text{den}_h(\mathcal{S}) = 12h(2r + 1)/n, \quad \text{den}(\mathcal{S}) = \lim_{h \rightarrow \infty} \text{den}_h(\mathcal{S}).$$

Only those having a limit are competitors for maximal density. But the limiting process is not without its problems. Given a CSP on $\text{Cyl}(r)$ with maximal density, one can randomly remove any billion spheres and what is left has equal density. So in practice one searches for packings which follow some motif that seems to optimize pre-densities. The search process is tricky to justify, computing pre-densities is difficult, and proving maximality is even harder. With the classical 2D/3D cases in mind, along with nature's apparent preferences, we are led to this conjecture. An affirmative answer, at least for small r , is posited in the physics literature [9,10], but a mathematical justification remains to be found.

Conjecture 2. *If $\text{Cyl}(r)$ supports a hexagonal cylindrical sphere packing \mathcal{S} , then \mathcal{S} has the maximal density among all sphere packings on $\text{Cyl}(r)$.*

There is one case in which we can affirm this conjecture, if you are willing to treat the plane as a cylinder with infinite radius. The solid cylinder is now the slab of space between planes $z = 0$ and $z = 1$. Maximality of the hexagonal packing of spheres within this slab follows easily from maximality of the penny packing in the 2D case. The slab is the union of the Voronoi cells of the sphere centers, the Voronoi cell of a sphere center consisting of all points closest to that center than to any other. The global density is identical to the density of a sphere within its cell.

$$\frac{\text{Sphere volume}}{\text{Cell volume}} = \frac{6/(4\sqrt{3})}{\pi/6} \sim 0.6045997881.$$

As $m + n$ grows and the cylinder $\text{Cyl}(r)$ associated with the (m, n) -hCSP \mathcal{S} grows, the density of \mathcal{S} will converge to this value, roughly 60%. I ask the reader to test their intuition: Is the density of an (m, n) -hCSP larger or smaller than 60%? The intuition of the author failed on this question, but the reader can settle the issue with data provided in §. As to proofs, § also presents some evidence for the

(m, m) -hCSP cases of the Conjecture. The approach is limited, however, and even for these limited cases the arguments remain incomplete.

As for the general situation, most cylinders $\text{Cyl}(r)$ do not support hCSP's, and the density question becomes much more difficult. In the physics literature the parameter D/d is varied continuously in simulations, and hCSP's emerge only for isolated values. For other values, hexagonal close packing still seems to be nature's preference, but with spiral patterns of gaps — what are called *line-slip* packings.

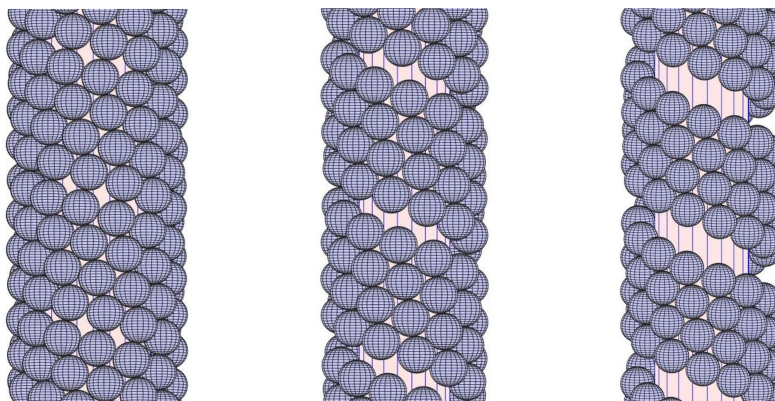


Figure 10. Line-slip packings: largely hexagonal, but with spiral gaps.

This figure illustrates cylinders of three different radii, so we are not comparing their densities. Rather, note that while packing (a) would appear to be rigid, it has spheres which are tangent to just 5 neighbors. As for packings (b) and (c), these have open gaps and appear to be somewhat flexible. However, with its smaller gap, it would seem difficult to add any spheres to (b), whereas with (c) one can conceive of adjustments that would allow additional spheres and thus perhaps larger density.

Part D: Computations

The developments and claims in Parts A, B, and C depended on the reader's familiarity with spheres, cylinders, and triangles and on their ability to carry out and visualize manipulations. Now it is time to back up this work with mathematical rigor.

First some general and standard background facts. Isometries of \mathbb{R}^3 are homeomorphisms which preserve euclidean distance, hence they preserve cylinders, spheres, and flat triangles. In the sequel we restrict attention to cylinders with central axis the z -axis and to isometries that map the z -axis to itself, and hence map CSP's to CSP's. They are generated by combinations of translations in the z -direction, rotations about the z -axis, and reflections in the coordinate planes. We can apply an isometry to move any sphere of a CSP so its center is on the positive x -axis, as we have done with the base sphere S_0 . A useful observation for later is that given any two points on a common cylinder, there is an isometry which interchanges those two points.

D.1. Smallest cylinder

Our definition of CSP allows the cylinder $\text{Cyl}(r)$ to have any radius $r \geq 0$. However, we are interested in hexagonal flowers. When $r = 0$ the attached spheres must all touch the z -axis, and the best one can hope for is shown in Figure 11(a). This may look promising until you note that flowers have only 5 petals, one exactly opposite the central sphere. Problems persists briefly as r gets larger. One might be led to the CSP of Figure 11(b), where $r \sim 0.0303300857$ and $\zeta = -1/2$. Base S_0 and the spheres directly above and below do have hex flowers, but as the view from the back shows in Figure 11(c), the other spheres have room for only five neighbors.

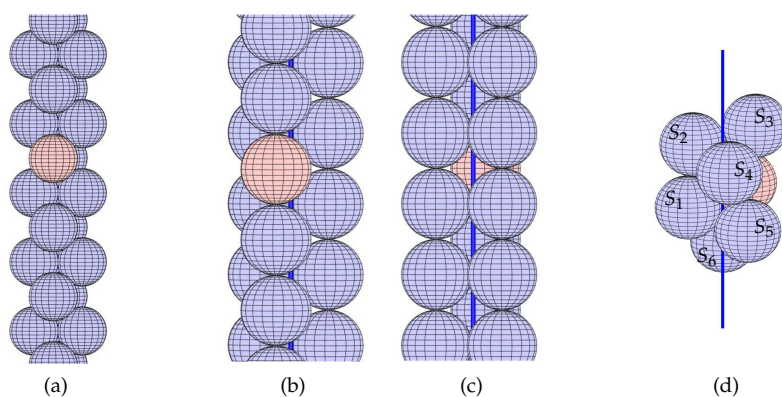


Figure 11. Search for the smallest cylinder.

A close look at Figure 11(c) will note gaps that are ringed by four spheres. These suggest room for improvement. Decreasing ζ from the initial value $-1/2$ introduces a twist, and as you know if you have ever played with a rope — twisting makes it smaller around. Here the twisting ends with the CSP of Figure 11(d), having $\zeta \sim -0.31619807367$. At this point, the opposite petals S_1 and S_4 are tangent to one another, so it is clear that we can not decrease r any further.

Lemma 1. *The minimum radius r for which $\text{Cyl}(r)$ supports a hex flower is $r \sim 0.0196290419$. Moreover, this hex flower extends to an hCSP, namely, the $(2, 1)$ -hCSP shown in Figure 1.*

In the notation we have adopted, this minimal radius is denoted $r(2, 1)$. Henceforth we assume our cylinders have radius $r \geq r(2, 1)$.

D.2. Hex Flower Closure

It is evident physically when working with a real life cylinder and real life (uniform) spheres, that if you position a sphere, place a tangent petal sphere, and then successively add additional tangent spheres, a hex flower will result — that is, as you place the sixth sphere, it will be precisely tangent to the first sphere. We now prove this.

Lemma 2. *Suppose that $r \geq r(2, 1)$, that S is a sphere attached to $\text{Cyl}(r)$, and that S_1 is a sphere tangent to S . If spheres $\{S_2, S_3, S_4, S_5, S_6, S_7\}$ are successively tangent spheres placed about S , then S_7 is identical to S_1 .*

Proof. Without loss of generality, we may assume that S is centered at $(R, 0, 0)$ while S_j is centered at (R, θ_j, z_j) , $j = 1, 2, \dots, 7$. We will show that $\theta_4 = -\theta_1$ and $z_4 = -z_1$. Repeating that argument will show that $\theta_7 = -\theta_4$ and $z_7 = -z_4$, and hence S_7 is identical to S_1 .

The argument depends on a study of equilateral triangles (all unit-sided in the following). Denote by t_j the triangle formed by centers of the tangent triple $\{S, S_j, S_{j+1}\}$. Let e_j be the line segment between (the centers of) S and S_{j+1} . This is an edge shared by t_j and t_{j+1} , and it is evident that these are the only equilateral triangles with vertices on $\text{Cyl}(R)$ which have e_j as an edge.

We refer to t_{j+1} as the *reflection* of t_j in e_j . The justification lies with an observation we made earlier: there is an isometry T that maps $\text{Cyl}(R)$ to itself and interchanges S and S_{j+1} . This clearly interchanges t_j and t_{j+1} , and therefore $S_{j+2} = T(S_j)$. The change in angle (the θ coordinate) from S_{j+1} to S_{j+2} is the negative of the change in angle from S to S_j , which is θ_j . We conclude that $\theta_{j+2} = \theta_{j+1} - \theta_j$. Likewise with heights, $z_{j+2} = z_{j+1} - z_j$. Reflecting in, successively t_1 and t_2 , we have successive the expressions

$$\theta_3 = \theta_2 - \theta_1, \quad z_3 = z_2 - z_1, \quad \theta_4 = \theta_3 - \theta_2, \quad z_4 = z_3 - z_2.$$

In consequence,

$$\theta_4 = \theta_2 - \theta_1 - \theta_2 = -\theta_1 \text{ and } z_4 = z_2 - z_1 - z_2 = -z_1.$$

Repeating by reflecting in t_4 and then in t_5 , we have $\theta_7 = -\theta_4 = \theta_1$ and $z_7 = -z_4 = z_1$. In other words, S_7 equals S_1 . \square

This result confirms our observations about the three spiral paths within an hCSP; see Figure 5. In each path one enters a flower via (the center of) one petal, passes through the central sphere, and exits via the opposite petal. Now we see that the increments in angle and height in each step are identical, implying that those centers lie on a common helix. Of course, in an $(m, 0)$ -hCSP, one path degenerates to a closed ring, while in an (m, m) -hCSP, one path degenerates to an infinite vertical path.

D.3. Universal covers

It is well known that the plane is the universal cover for a cylinder. In studying sphere packings on a given cylinder $\text{Cyl}(r)$, the centers are given in cylindrical coordinates by (R, θ, z) , where $R = r + 1/2$. Since only the coords θ and z vary, it is convenient to define a universal covering map $\Phi_R : (\theta, z) \mapsto (R, \theta, z)$ from the (θ, z) -plane onto the mid cylinder $\text{Cyl}(R)$. This is 2π periodic in the first coordinate, so $\Phi_R(\theta + 2\pi, z) = \Phi_R(\theta, z)$. A convenient fundamental domain is the strip $\{(\theta, z) : 0 \leq \theta < 2\pi\}$.

Using Φ_R , spheres attached to $\text{Cyl}(r)$ may be identified with their “centers” as points in the (θ, z) -plane. Given a hex flower on $\text{Cyl}(r)$, geodesics between centers on $\text{Cyl}(R)$ lift to straight lines, so on the plane that hex flower defines three straight line segments. We are now in position to formalize the general hex construction undertaken in §A.2. by working in the (θ, z) -plane.

Constructions started with base sphere S_0 centered at $(0, 0)$ and a tangent sphere S_1 centered at (θ_1, z_1) . We then computed S_2 tangent to S_0 and S_1 , with center (θ_2, z_2) . Define the vectors $\bar{u} = \langle \theta_1, z_1 \rangle$ from (the center of) S_0 to S_1 , $\bar{v} = \langle \theta_2, z_2 \rangle$ from S_0 to S_2 , and $\bar{w} = \bar{v} - \bar{u} = \langle \theta_2 - \theta_1, z_2 - z_1 \rangle$ from S_1 to S_2 . The six centers about $(0, 0)$ are in the directions $\{\bar{u}, \bar{v}, \bar{w}, -\bar{u}, -\bar{v}, -\bar{w}\}$. The construction continues by successively adding neighbors to complete the hex flower of any existing sphere. Proceeding *ad infinitum* in the plane, we generate the hexagonal lattice

$$\Lambda = \{a\bar{u} + b\bar{v} : (a, b) \in \mathbb{Z}^2\}.$$

In the generic situation, projecting these points to centers on a mid cylinder $\text{Cyl}(R)$ will lead to distinct centers that are too close — their spheres would not have disjoint interiors. This can only be avoided if Λ is 2π -periodic.

Lemma 3. *Given $\text{Cyl}(r)$, tangent spheres S_0, S_1 generate an hCSP on $\text{Cyl}(r)$ if and only if the associated lattice Λ is 2π -periodic, if and only if Λ contains $(2\pi, 0)$, if and only if there exist integers m, n so that $m\bar{u} + n\bar{v} = (2\pi, 0)$.*

Figure 12 illustrates the situation for the $(7, 3)$ -hCSP: • the lattice Λ with edges for tangencies • the shaded fundamental domain • the spiral through S_0, S_1 in red • the spiral through S_0, S_2 in green • the spiral through S_0, S_3 in blue • the covering map • the projection to the mid cylinder $\text{Cyl}(R)$.

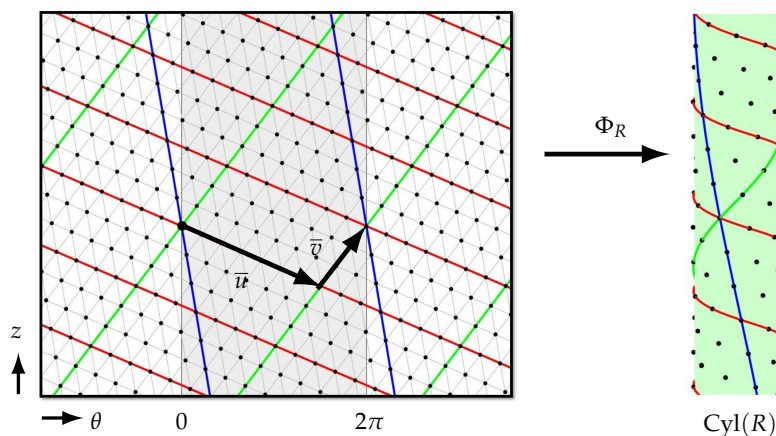


Figure 12. The lattice Λ for the $(7,3)$ -hCSP covering the mid cylinder.

In this figure, one can see a concrete meaning for m and n : the full lattice is formed by $m = 7$ parallel copies of the green spiral or $n = 3$ copies of the red spiral. Though harder to see, it is formed as well by $l = m + n = 10$ copies of the blue spiral. In biological studies of plant growth, 3-tuples (l, m, n) are known as *parastichy* numbers and arise in the context of *phyllotaxis*, the growth of spiral patterns in plants, such as sunflowers, pine cones, or corn. (See [7,10].) We will stick with our (m, n) notation.

A cautionary note about covering maps: Φ_R is not the classical textbook covering map — the covering map used, e.g., in the related physics literature (see [10]). It differs by a scaling by factor R in the first variable, so infinitesimal distances in the plane and the mid cylinder are not equal (except for the $(6,0)$ -hCSP, in which case $R = 1$). Neither is Φ_R the covering map discussed in relation to Figure 8, which is actually covering an underlying polyhedral cylinder.

Lemma 3 confirms the second statement in Theorem 1. However, this approach is not helpful in proving the first statement, so in the next subsection we prove the mathematical details to support that part of our proof.

D.4. Monotonicity Results

We confirm various claims made about necklaces on cylinders $\text{Cyl}(r)$ in the proof of Theorem 1. Integers m and n are given with $m > n > 0$. We search for appropriate geometric parameters r and ζ by considering (m, n) -elegant necklaces in the covering lattice described above: the first m sphere centers are incremented by the lattice vector $\bar{u} = \langle \theta_1, \zeta \rangle$ while the remaining n are incremented by $\bar{v} = \langle \theta_2, z_2 \rangle$, with $\zeta \leq 0$ and $z_2 > 0$. Two key equations reflect the fact that a necklace must be closed:

- (a) Height closure: $m\zeta + nz_2 = 0$.
- (b) Angle closure: $m\theta_1 + n\theta_2 = 2\pi$.

Height closure implies $z_2 = -(m/n)\zeta$, meaning we can eliminate z_2 in subsequent expressions. The radius r enters because when moving between tangent spheres on $\text{Cyl}(r)$ the increments in angle θ and in height z are related. Specifically

$$\theta = \arccos\left(1 - \frac{(1 - z^2)}{2R^2}\right), \quad R = r + 1/2.$$

Computation gives

$$\frac{\partial\theta}{\partial z} = \frac{-z}{R^2 \sin(\theta)}, \quad \frac{\partial\theta}{\partial R} = \frac{\partial\theta}{\partial r} = \frac{-(1 - z^2)}{R^3 \sin(\theta)},$$

meaning that the angles are decreasing as functions of $|z|$ and of r .

Consider an (m, n) -elegant necklace on $\text{Cyl}(r)$. We claimed in our proof of Theorem 1 that this necklace is unique. If ζ were to become more negative, then both $|\zeta|$ and $|z_2| = (m/n)|\zeta|$ would increase, implying both θ_1 and θ_2 would decrease, contradicting the angle closure condition. Likewise, if ζ were to become less negative, both $|\zeta|$ and $|z_2|$ would decrease, θ_1 and θ_2 would increase, again contradicting the angle closure condition. Thus there is only one (m, n) -elegant necklace on $\text{Cyl}(r)$ and hence only one associated height increment ζ .

Next, applying implicit differentiation to the angle closure condition (b) gives

$$\frac{d\zeta}{dR} = -\frac{m(1-\zeta^2)\sin(\theta_2) + n(1-(m/n)^2\zeta^2)\sin(\theta_1)}{Rm\zeta[\sin(\theta_2) + (m/n)\sin(\theta_1)]}.$$

Since $\zeta < 0$, the expression for $\frac{d\zeta}{dR}$ is positive. Therefore, as we have claimed, when the radius r of the cylinder decreases, then the height $m\zeta$ of the lowest sphere S of the (m, n) -elegant necklace decreases — i.e., the necklace droops lower.

We showed by the intermediate value theorem that there is some radius r so that $\text{Cyl}(r)$ supports an (m, n) -Goldilocks necklace. The final claim to verify is that this r is unique. Recall that this involved the lowest sphere, S , in (m, n) -elegant necklaces along with two tangent spheres (see Figure 7). The first of these, S_G , is displaced from S at $\langle 0, 0 \rangle$ by the vector $\bar{u} = \langle \theta_1, \zeta \rangle$ and the second by vector $\bar{v} = \langle \theta_2, z_2 \rangle$. Let $\alpha(r)$ be the angle at S in the triangle formed by these three and let $C(R) = \cos(\alpha(r))$, a function of $R = r + 1/2$. It suffices to show that $dC/dR > 0$.

Applying an isometry we may assume S is centered at $(R, 0, 0)$, S_G at (R, θ_1, ζ) , and S_B at (R, θ_2, z_2) . In euclidean coordinates, the 3D vectors from S to S_G and to S_B are, respectively, the unit vectors

$$\bar{U} = (R - R\cos(\theta_1), R\sin(\theta_1), \zeta), \quad \text{and} \quad \bar{V} = (R - R\cos(\theta_2), R\sin(\theta_2), z_2).$$

Let us agree to some abbreviations: $c_j = \cos(\theta_j)$ and $s_j = \sin(\theta_j)$, for $j = 1, 2$, and also $c_{12} = \cos(\theta_1 - \theta_2)$ and $s_{12} = \sin(\theta_1 - \theta_2)$. These will greatly facilitate the computations involving $C(R)$.

$$\begin{aligned} C(R) &= \bar{U} \cdot \bar{V} = R^2(c_1 - 1)(c_2 - 1) + R^2s_1s_2 + \zeta z_2 \\ &= R^2(1 - c_1 - c_2) + R^2c_{12} - (m/n)\zeta^2 \\ &= 1 - R^2 - \left(\frac{m^2 + n^2}{2n^2}\right)\zeta^2 + R^2c_{12} - (m/n)\zeta^2 \\ &= 1 - R^2 - \left(\frac{(m+n)^2}{2n^2}\right)\zeta^2 + R^2c_{12}. \end{aligned}$$

Computing the derivative, we see

$$\begin{aligned} \frac{dC}{dR} &= -2R - \left(\frac{(m+n)^2}{n^2}\right)\zeta \frac{d\zeta}{dR} + R^2s_{12}\left(\frac{d\theta_2}{dR} - \frac{d\theta_1}{dR}\right) + 2Rc_{12} \\ &= -2R + \left(\frac{(m+n)^2}{mn}\right) \frac{m(1-\zeta^2)s_2 + n(1-(m/n)^2\zeta^2)s_1 + (m-n)s_{12}}{R(ns_2 + ms_1)} \\ &\quad + 2Rc_{12}. \end{aligned}$$

Note that $\theta_2 \leq \theta_1 \leq 2\theta_2$, so $(\theta_2 - \theta_1) < \theta_2$. We get the inequalities $s_2 \leq s_1 \leq 2s_2$ and $c_{12} \geq c_2$, and in turn,

$$2Rc_{12} \geq 2Rc_2 = 2R\left(1 - \frac{1 - (m/n)^2\zeta^2}{2R^2}\right) = 2R - \frac{(1 - (m/n)^2\zeta^2)}{R}.$$

Now we note a succession of inequalities:

$$\begin{aligned}
 \frac{dC}{dR} &\geq \left(\frac{m+n}{mn}\right) \frac{(m(1-\zeta^2)s_2 + n(1-(m/n)^2\zeta^2)s_1)}{R(ns_2 + ms_1)} - \frac{(1-(m/n)^2\zeta^2)}{R} \\
 &> \left(\frac{m+n}{mn}\right) \frac{(m(1-(m/n)^2\zeta^2)s_2 + n(1-(m/n)^2\zeta^2)s_1)}{R(ns_1 + ms_1)} - \frac{(1-(m/n)^2\zeta^2)}{R} \\
 &> \left(\frac{m+n}{mn}\right) \frac{(m+n)(1-(m/n)^2\zeta^2)s_2}{R(m+n)s_1} - \frac{(1-(m/n)^2\zeta^2)}{R} \\
 &= \left(\frac{m+n}{mn}\right) \frac{(1-(m/n)^2\zeta^2)}{2R} - \frac{(1-(m/n)^2\zeta^2)}{R} \\
 &> 0.
 \end{aligned}$$

This is what we wanted to show: the fact that $dC/dR > 0$ implies that there will be only one cylinder $Cyl(r)$ supporting an (m, n) -Goldilocks necklace. This completes the details for the claims we made in the proof of Theorem 1.

That brings us to the practical problem of finding the values of r and ζ for a given pair (m, n) . We noted earlier the explicit solutions for cases $(m, 0)$ and (m, m) , but to the author’s knowledge there are no other explicit solutions. The approach to the proof of Theorem 1, wherein the value of r is decreased until an (m, n) -Goldilocks necklace is found, can be implemented numerically. This table provides approximate values for values of r for m in the range 2 to 13.

Table 1. Cylinder radii for (m, n) -hCSP’s, $m = 2, \dots, 13$.

$m \setminus n$	0	1	2	3	4	5	6
2	*	0.0196290419	0.1123724357				
3	0.0773502692	0.1452616461	0.2431283644	0.3660254038			
4	0.2071067812	0.2856098969	0.3846240416	0.5018804956	0.6315167192		
5	0.3506508084	0.4325849755	0.5311569265	0.6444141170	0.7688700797	0.9012585384	
6	0.5	0.5831845450	0.6807569165	0.7908960515	0.9111728813	1.0392003480	1.1730326075
7	0.6523824355	0.7359998206	0.8324219685	0.9399926944	1.0568342905	1.1811092662	1.3112354268
8	0.8065629649	0.8902678585	0.9855566370	1.0909457796	1.2049023274	1.3259498048	1.4527672542
9	0.9619022001	1.0455414663	1.1397724649	1.2432804142	1.3547712360	1.4730137330	1.5969015931
10	1.1180339887	1.2015408950	1.2948084394	1.3966743006	1.5060242195	1.6218126006	1.7430843299
11	1.2747327664	1.3580813817	1.4504786749	1.5508976867	1.6583736322	1.7719955302	1.8909327960
12	1.4318516526	1.5150326938	1.6066469807	1.7057899444	1.8116080132	1.9233014648	2.0401412351
13	1.5892907344	1.6723076354	1.7632209762	1.8612236940	1.9655605867	2.0755248045	2.1904720432
$m \setminus n$	7	8	9	10	11	12	13
7	1.4459414186						
8	1.5842617208	1.7195498855					
9	1.7254702745	1.8579272334	1.9936207664				
10	1.8690058043	1.9988486482	2.1320179590	2.2680134412			
11	2.0144434561	2.1418868738	2.2726988110	2.4064189762	2.5426391734		
12	2.1614633356	2.2866935874	2.4153065939	2.5468806365	2.6810370913	2.8174391632	
13	2.3098049512	2.4329930196	2.5595707414	2.6891317304	2.8213209281	2.9558226383	3.0923728858

There are some patterns in the data that confirm your intuition. As you might expect, the values are increasing across rows and down columns. As m grows, r grows, so $Cyl(r)$ has less and less curvature, and the packing looks increasing like the hexagonal close packing of spheres attached to a plane, $Cyl(\infty)$. Intuition about twisted ropes leads to a more subtle pattern: As you more tightly twist a rope, we expect to see its diameter decreasing. Consider elegant pearl necklaces with the same number of pearls, say, for example, 12 pearls as in Figure 13. As n grows at the expense of m , the height increment ζ becomes more negative, the twist is more visually evident, and the cylinder radius decreases. The table entries suggest that $r(m - 1, n + 1)$ is less than $r(m, n)$ — in other words, you see r increasing as you move up and to the right in the table. This is an observation not a proof, but is supported by intuition.

D.5. About Density

Has the reader made their best guess about packing density for hCSP’s? Is the density greater or smaller than the roughly 60% achieved by the hexagonal sphere packing on a plane? This table

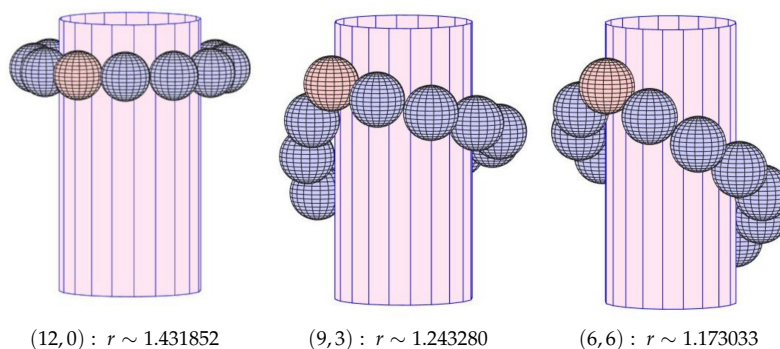


Figure 13. Twelve-pearl necklaces: More twist means a smaller cylinder?

provides a sampling of approximate densities; aside from the $(2, 1)$ case, I have chosen $(m, 0)$ -hCSP's for consistency.

Table 2. Representative densities for hCSP's.

(m, n)	(2,1)	(3,0)	(4,0)	(5,0)	(10,0)	(50,0)	(100,0)	(300,0)	$(\infty, 0)$
r	0.01963	0.07735	0.20711	0.35065	1.11803	7.46299	15.418112	47.247355	∞
density	0.50714	0.53033	0.56060	0.57582	0.59721	0.60430	0.60453	0.60459	0.60460

Turning now to the density Conjecture 2, it seems plausible that this is true in the limited case of (m, m) -hCSP's. Here is a potential line of reasoning. Suppose \mathcal{S} is an (m, m) -hCSP on $\text{Cyl}(r)$, some $m \geq 2$ and we wish to compare its density to that of \mathcal{S}' , a CSP on the same cylinder. The direct approach would compare the numbers V and V' of spheres in truncated cylinders. Such counting may be straightforward for \mathcal{S} , but it is likely more involved for \mathcal{S}' . We suggest, instead, moving to consideration of triangulations T and T' formed by the centers.

How do triangulations help? Truncations of T and T' to heights $[-h, h]$ will be triangulations of an annulus, hence with euler characteristic $V - E + F = 0$. The number E_{∂} of boundary edges is clearly bounded above independent of h , while V and E and F grow without bound. Counting edges by faces gives

$$E = 3F/2 + E_{\partial} \implies V = F/2 + E_{\partial} \implies V \sim F/2. \quad (3)$$

In light of this, we can compare the numbers of faces rather than the numbers of vertices in the truncated triangulations. And we might do this indirectly by looking at the face areas.

We lift T and T' under the covering map Φ_R so we can work in the plane, that is, in the (θ, z) -plane as described in §D.3.. The triangles in the plane correspond to geodesic triangles on $\text{Cyl}(R)$, and their euclidean areas are proportional to surface areas, with scaling factor $1/R$. We may be able to avoid counting by comparing areas: if the areas of triangles of T are no bigger than those of T' , then the number of faces in a truncated portion of the triangulations will be no smaller, and we would conclude that $\text{den}(\mathcal{S}) \geq \text{den}(\mathcal{S}')$, as conjectured.

A triangle in the plane will be called "special for R " if the lifts of its three vertices under Φ_R determine a unit-sided equilateral triangle inscribed in $\text{Cyl}(R)$ (i.e., so the lifted vertices are centers for a tangent triple of spheres; see, e.g., Figure 2.) Among the special triangles for R , there is only one (up to translations and horizontal flips) which has a side that is vertical. (Its projection to $\text{Cyl}(R)$ is also vertical and has geodesic length 1). We will denote this triangle by Δ_R . One can show that for any R , Δ_R has area strictly smaller than any other special triangle for R .

We return to our triangulations T and T' . As \mathcal{S} is an (m, m) -hCSP, all its faces are copies of Δ_R . If we assume for a moment that the competing packing \mathcal{S}' is also hexagonal, the faces in T' would all have areas strictly larger than those of T . Without knowing anything further about the triangulations, we can conclude that the number of triangles in T will outrun the number in T' , implying *via* (3) that $\text{den}(\mathcal{S}) \geq \text{den}(\mathcal{S}')$. Of course, existence of such a \mathcal{S}' would provide a positive answer to Open

Question 1. So what of more general competitors S' ? One is tempted to posit that the area for faces of T is smallest in other situations.

Open Question 3. If t is a triangle in the (θ, z) -plane whose corners lift to points on $\text{Cyl}(R)$ at least euclidean distance 1 apart from one another, is the area of t greater than or equal to the area of the special triangle Δ_R ?

A positive answer would ensure that S has maximal density among all CSP's on $\text{Cyl}(r)$. It is tempting to exploit some extremal property of equilateral triangles, but note that Δ_R is not itself an equilateral triangle, nor is the corresponding geodesic triangle on $\text{Cyl}(R)$ equilateral — at least two of its geodesic sides are length greater than 1.

Finally, note that this particular approach only applies when S is an (m, m) -hCSP. Other situations seem to require much more detailed analysis, perhaps like that employed by Hales [6], to understand the excluded volume. One might start by breaking the solid cylinder into Voronoi cells associated with the sphere centers: these cell would be bounded by planes and parts of the inner and outer cylinders. In any case, there seem to be interesting new questions here and perhaps some of them will capture the reader's attention.

Acknowledgments: During the preparation of this manuscript, the author used *Matlab*(R2025b) and *CirclePack* <https://github.com/kensmath/CirclePack> for computations and *Matlab* for images. The author has reviewed the output and takes full responsibility for the content of this publication.

Conflicts of Interest: The author declares no conflicts of interest.

References

1. Beardon, A.F.; Dubejko, T.; Stephenson, K. Spiral hexagonal circle packings in the plane. *Geometriae Dedicata* **1994**, *49*, 39–70.
2. Chan, H.K.; Winkelmann, J. *Columnar Structures of Spheres: Fundamentals and Applications*; Jenny Stanford Publishing: Singapore, 2023.
3. Cohn, F.; Kumar, A.; Miller, S.D.; Radchenko, D.; Viazovska, M. The sphere packing problem in dimension 24. *Annals of Mathematics* **2017**, *185* (3), 1017–1033.
4. Conway, J.; Sloane, N.J.A. *Sphere packings, lattices and groups, 3rd Ed.*; Springer: New York, 1999.
5. Graver, J.; Servatius, B.; Servatius, H. Combinatorial rigidity. *Graduate Studies in Math.* **2** **1993**; Amer. Math. Soc.
6. Hales, T.C. A proof of the Kepler conjecture. *Ann. of Math.* **2005**, *162*, 1065–1185.
7. Levitov, L.S. Fibonacci numbers in botany and physics: Phyllotaxis. *JEPT Letters* **1991**, *54*, 542.
8. Mughal, A.; Chan, H.K.; Weaire, D. Phyllotactic Description of Hard Sphere Packing in Cylindrical Channels. *Phy. Rev. Letters* **2011**, *106*, 115704.
9. Mughal, A. Screw symmetry in columnar crystals. *Philosophical Magazine* **2013**, *93*:31=33, 4070–4077.
10. Mughal, A.; Weaire, D. Theory of cylindrical dense packings of disks. *Phy. Rev. E* **2014**, *89*, 040307.
11. Rodin, B.; Sullivan, D. The convergence of circle packings to the Riemann mapping. *J. Differential Geometry* **1987**, *26*, 349–360.
12. Stephenson, K. *Introduction to Circle Packing: the Theory of Discrete Analytic Functions*; Camb. Univ. Press: New York, 2005. (ISBN 0-521-82356-0, QA640.7.S74).
13. Thurston, W. The finite Riemann mapping theorem, 1985. Invited talk, An International Symposium at Purdue University in celebrations of de Branges' proof of the Bieberbach conjecture, March 1985.

Disclaimer/Publisher's Note: The statements, opinions and data contained in all publications are solely those of the individual author(s) and contributor(s) and not of MDPI and/or the editor(s). MDPI and/or the editor(s) disclaim responsibility for any injury to people or property resulting from any ideas, methods, instructions or products referred to in the content.